Journal of the European Ceramic Society **12** (1993) 271–277

Microstructure and Thermal Conductivity of $AlN(Y_2O_3)$ Ceramics Sintered in Different Atmospheres

H. Buhr* & G. Müller‡

Technische Hochschule Darmstadt, Fachbereich Materialwissenschaft, Fachgebiet Nichtmetallisch-Anorganische Werkstoffe, Schnittspahnstraße 9, D-6100 Darmstadt, Germany

(Received 24 August 1992; revised version received 10 March 1993; accepted 31 March 1993)

Abstract

Thermal conductivity, microstructure and oxygen content in the AlN lattice of $AlN(Y_2O_3)$ ceramics, made of different AlN powders and prepared by either pressureless sintering in a graphite-heated furnace (type I samples) or sintered in a graphite-free furnace (type II samples), have been investigated. In the type I samples the secondary phases are present as a continuous network along the AlN grain edges, whereas they form isolated lumps in the type II samples. For these two types of microstructure simple models are presented which allow calculation of thermal conductivity as a function of the oxygen content dissolved in the AlN lattice and as a function of microstructural parameters (amount of secondary phases, thickness of layers between neighbouring AlN grains). The calculated conductivities are in good agreement with the measured values, the deviations found are typically < 15 W/(m K). As a result, it is shown that the oxygen content dissolved in the AlN lattice has the dominating influence in AlN ceramics having an amount of secondary phases < 10 vol.% and amorphous layers with a thickness of typically 2–4 nm between neighbouring AlN grains.

Die Wärmeleitfähigkeit, das Gefüge und der im AlN-Korn gelöste Anteil an Sauerstoff von $AlN(Y_2O_3)$-Keramiken wurden untersucht. Die Keramiken wurden aus unterschiedlichen AlN-Pulvern hergestellt und entweder in einem graphitbeheizten (Proben Typ I) oder graphitfreien Ofen (Proben Typ II) drucklos gesintert. In den Proben des Typs I lagen die Nebenphasen in Kanälen entlang der AlN-Kornkanten vor, in den Proben des Typs II dagegen als einzelne, isolierte Körner. Für diese unterschiedlichen Arten der Gefügeausbildung wird mit Hilfe einfacher Gefügemodelle die Wärmeleitfähigkeit als Funktion des im AlN-Korn gelösten Sauerstoffgehalts und der Dicke von amorphen Belegungen auf den AlN–AlN-Kornkontaktflächen berechnet. Die berechneten Wärmeleitfähigkeiten stimmen gut mit den gemessenen überein, die Abweichungen sind typisch < 15 W/(m K). Die Untersuchungen zeigen, daß der im AlN-Korn gelöste Sauerstoffgehalt den entscheidenden Einfluß auf die Wärmeleitfähigkeit von AlN-Keramiken hat, wenn der Anteil an Nebenphasen < 10 Vol.% ist und die Dicke der AlN–AlN-Kornflächenbelegungen etwa 2–4 nm beträgt.

On a étudié la conductivité thermique, la microstructure et la teneur en oxygène dans le réseau d'AlN de céramiques $AlN(Y_2O_3)$, faites à partir de différentes poudres d'AlN et préparées par frittage sous pression normale soit dans un four à éléments chauffant en graphite (échantillons de type I), soit dans un four sans graphite (échantillons de type II). Dans les échantillons de type I les phases secondaires sont présentes sous forme d'un réseau continu le long des grains d'AlN, alors que dans les échantillons de type II elles se retrouvent sous forme d'agglomérats. On a présenté pour ces deux types de microstructure des modèles simples, qui permettent le calcul de la conductivité thermique en fonction de la teneur en oxygène dissout dans le réseau cristallin d'AlN et des paramètres microstructuraux (quantité de phases secondaires, épaisseur des couches entre les grains d'AlN voisins). Les conductivités thermiques calculées sont en bon accord avec les valeurs mesurées; les différences trouvées sont typiquement < 15 W/(m K).

* Present address: Metallgesellschaft AG, Reuterweg 14, D-6000 Frankfurt, Germany.

‡ Present address: Fraunhofer-Institut für Silicatforschung, Neunerplatz 2, D-8700 Würzburg, Germany.

Journal of the European Ceramic Society 0955-2219/93/$6.00

Comme résultat, on a montré que la teneur en oxygène dissout dans le réseau d'AlN est le facteur dominant qui influence les céramiques AlN, ayant une quantité de phase secondaire < 10 vol.% et des couches amorphes d'une épaisseur typique de 2 à 4 nm entre les grains d'AlN voisins.

1 Introduction

Aluminium nitride (AlN) is a promising material, having a very high thermal conductivity. The thermal conductivity of pure AlN single crystals is 320 W/(m K) as calculated and 285 W/(m K) as measured.[1] It is known that this difference in thermal conductivity is due to impurities, particularly oxygen. As $Al_{0.67}O$ is dissolved in the AlN lattice, the mass defect of aluminium vacancies causes phonon scattering.[1,2]

Thermal conductivity of polycrystalline, multiphase AlN ceramics (100–200 W/(m K)) is considerably lower than that of AlN single crystals. It has been shown that the oxygen content dissolved in the AlN lattice has a strong influence on thermal conductivity in such ceramics.[3–5] Microstructural parameters, however, can also influence their thermal conductivity considerably.[6–9]

The aim of this work was to provide a quantitative correlation between thermal conductivity, the oxygen content in AlN lattice and microstructural parameters of AlN(Y_2O_3) ceramics.

2 Experimental Procedure

AlN powder grade F from Tokuyama Soda Co. Ltd, Tokyo, Japan with a mean particle size of 1·3 μm and an oxygen content of 0·85 wt%, called TSF, and Y_2O_3 powder from H. C. Starck, Berlin, Germany were used as standard starting materials. Additionally, three experimental AlN powders, called A, B and C, were used. These experimental powders had different oxygen contents: 1·4 wt% (A), 2·2 wt% (B) and 3·4 wt% (C). Total cationic impurities are below 200 ppm in all AlN powders: they are therefore thought to have only minor influence on the thermal conductivity of the samples. Mixtures of AlN with Y_2O_3 were made by attrition milling in 2-propanol. The dried powders were cold isostatically pressed into cylinders (23 mm diameter, 15 to 25 mm height) with a pressure of 300 MPa. The compacts were sintered in a gas pressure sintering furnace with graphite heating elements (graphite furnace) under a pressure of 0·2 MPa nitrogen. The heating rate was 30 K/min, the end temperature was 1800°C and sintering time was 3 h. These samples from the graphite furnace are called type I samples. Other samples were sintered in a graphite-free furnace equipped with Mo heating elements (called type II samples). Sintering was done in Mo crucibles under a flowing N_2/H_2 atmosphere (90 vol.% N_2, 10 vol.% H_2) at a temperature of 1800°C for 3 h.

The microstructure and amount of secondary phases were investigated by SEM (SEM 505, Philips, Eindhoven, Netherlands). The grain face layers between neighbouring AlN grains were investigated by TEM (CM 12, Philips, Eindhoven, Netherlands). The width of these grain face layers was determined by bright field images at high magnification and analysis of defocus series.[10] The oxygen content dissolved in the AlN lattice was determined by selective hot gas extraction analysis[11] (Leco TC 436, Leco, St Joseph, MI, USA). Thermal conductivity was measured by a static method according to DIN 51908. In this method the unknown sample is placed in series with a reference sample between two heat reservoirs held at constant temperature (20°C and 40°C). Heat flow and hence thermal conductivity are derived from the thermal gradient established in the reference sample, measured by means of thermocouples. Thermal conductivities in the range from 10 to 200 W/(m K) can be measured with an accuracy of 3%. A set of standard metal samples was used periodically for calibration.

3 Results and Discussion

3.1 Influence of oxygen and microstructure on thermal conductivity (modelling)

The type I samples have a microstructure that can be described as being formed by irregular face-connected AlN polyhedra with rounded edges (see double arrow in Fig. 1(b)). The rounded edges of neighbouring AlN grains form a channel system containing the oxide phases (Y aluminates, see arrows in Fig. 1, called grain edge phases). In all samples additional thin layers, called grain boundary phases, are found between the AlN polyhedra (see Fig. 2). This grain boundary phase has a thickness of typically 2–3 nm, as found by defocus analysis at the TEM. Dark field images show that this phase is amorphous and EELS investigations at the TEM show that this layer is mainly consisting of Al_2O_3.[12]

The microstructure of type I samples is modelled as simple periodic stacking of cubes (for the AlN grains) with bevelled edges and secondary phases in the channels along the grain edges forming prisms (grain edge phase). The grain boundary phase was modelled as thin layers between the surfaces of neighbouring cubes. One volume element of this model is shown in Fig. 3. The thermal conductivity of this microstructural model is then calculated in

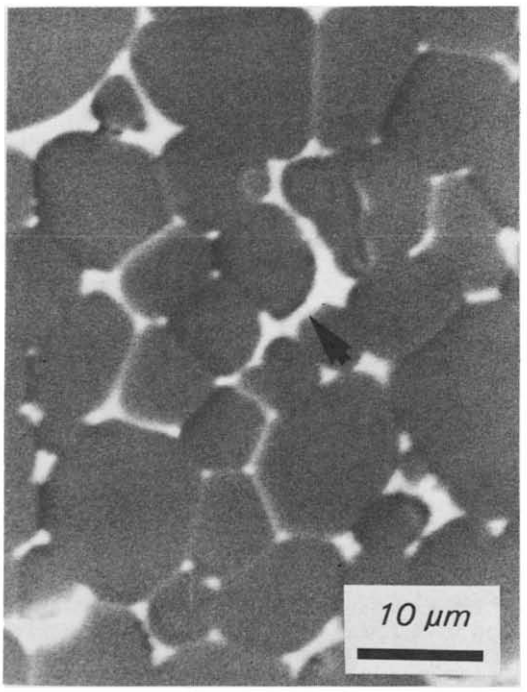

(a)

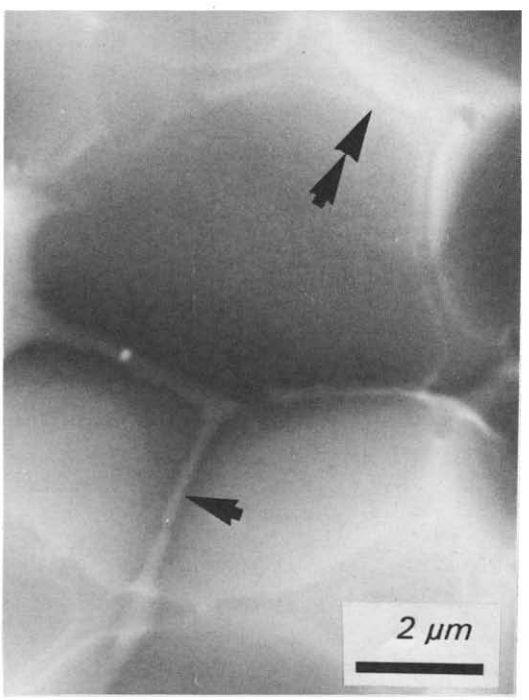

(b)

Fig. 1. SEM micrographs of AlN (3 wt% Y_2O_3) ceramic sintered in a graphite-heated furnace at 1800°C for 3 h. (a) Polished microsection with electron backscatter contrast between Y aluminates (arrow) and the AlN grains; (b) fracture surface showing that the Y aluminates (arrow) are formed along the AlN grain edges (double arrow).

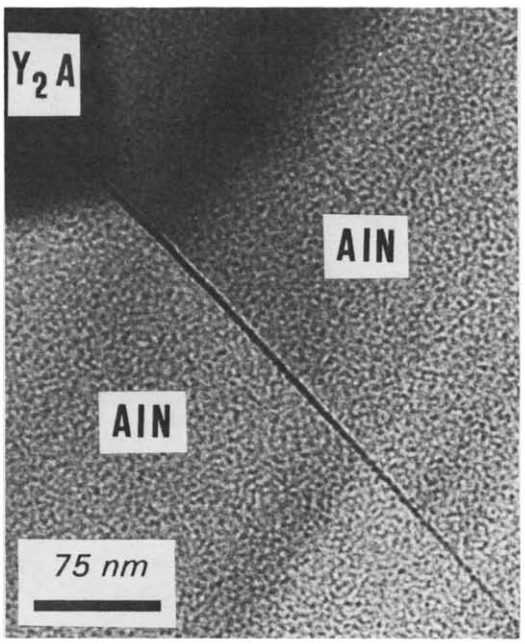

(a)

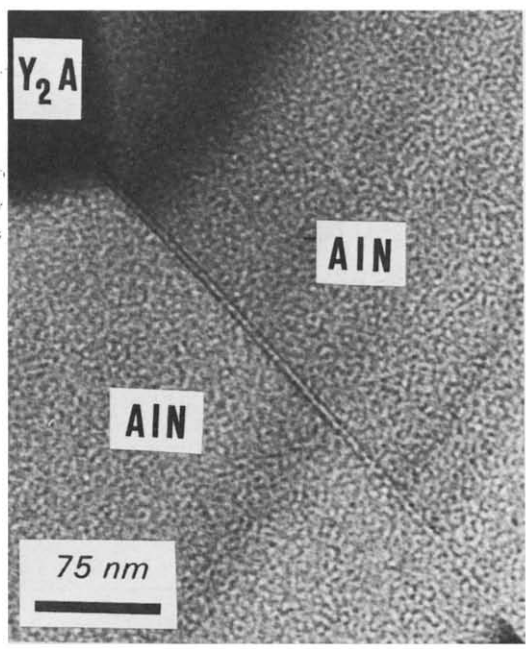

(b)

Fig. 2. (a) and (b) TEM micrographs of AlN (4 wt% Y_2O_3) ceramic sintered in a graphite-heated furnace showing layers of a few nm thickness between the AlN grain faces; the analysis of these defocus images (300 nm defocus) gives a layer thickness of 2·5 nm.

terms of Wiener's formulae[13] (see Appendix 1). These calculations are straightforward for the simple geometry of this model: the volume element (Fig. 3) is divided into its constituents and the thermal conductivity of each constituent is calculated. Total heat conduction (λ) is then derived from the sum of the heat flow. The resulting formula in a simplified form is given in Appendix 2. The variable parameters in the model calculations are: (1) amount of grain edge phase, (2) thickness of grain boundary phase, and (3) thermal conductivity of AlN given by the oxygen content dissolved in the AlN lattice. For the influence of oxygen content dissolved in the AlN lattice on thermal conductivity the correlation by Slack[2] was used because the present data are consistent with it.[3] For the thermal conductivities of the secondary phases values from the literature were used (10 W/(m K) for Y alumi-

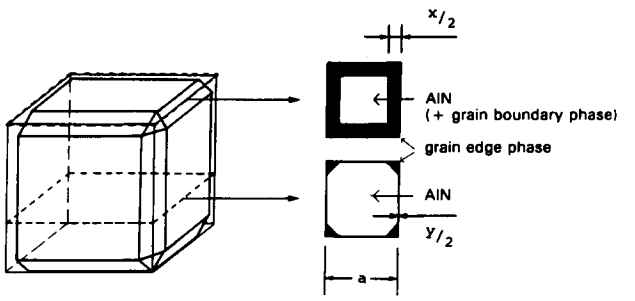

Fig. 3. Model of the microstructure of ceramics sintered in a graphite heated furnace.

nates, because the thermal conductivity of $Y_3Al_5O_{12}$ (YAG) is reported to be 11 W/(m K),[14] and 1 W/(m K) for the amorphous phase, because the thermal conductivity of a glass phase is approximately 1 W/(m K)). Selected results of these calculations are shown by the graphs in Figs 4 and 5; measured values of thermal conductivity, oxygen content in the AlN lattice and amount of secondary phases are listed in Table 1.

The microstructure of type II samples differs from that of type I inasmuch as the Y aluminates are concentrated in isolated grains (see arrows in Fig. 6) instead of forming interconnected channels. The TEM investigation shows that the type II samples also contain an amorphous, Al_2O_3-rich grain boundary phase with a thickness of typically 2–4 nm. The AlN grains with their grain boundary layers thus form a matrix that contains dispersed Y aluminate grains. The same type of microstructure was established in samples sintered in the graphite-heated furnace, but protected by an AlN powder bed in an AlN crucible. From this observation it seems

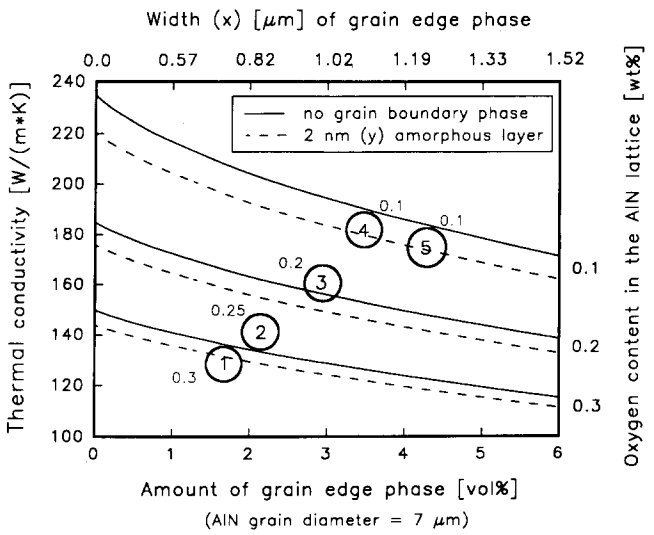

Fig. 4. Thermal conductivity as a function of the amount of grain edge phase. Parameters: oxygen content in the AlN lattice, width of grain boundary phase. Measured values: points 1–5 represent measured thermal conductivities and amount of grain edge phases of AlN ceramics with 1–5 wt% Y_2O_3 sintered at 1800°C for 3 h in a graphite-heated furnace. The figures beside the data points give the measured oxygen contents in the AlN lattice in wt%.

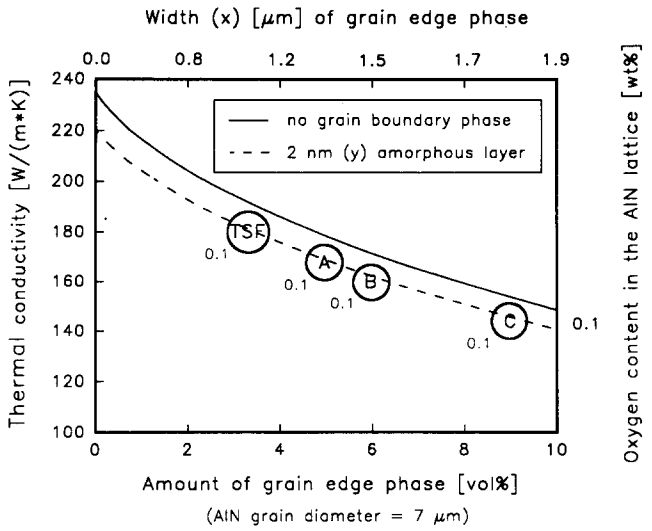

Fig. 5. Thermal conductivity as a function of the amount of grain edge phase. Parameters: oxygen content in the AlN lattice, width of grain boundary phase. Measured values: points TSF, A, B and C represent measured thermal conductivities and amount of grain edge phases of AlN ceramics made of different AlN powder and sintered at 1800°C for 3 h in a graphite-heated furnace. The figures beside the data points give the measured oxygen contents in the AlN lattice in wt%.

that differences in the furnace atmosphere (e.g. oxygen partial pressure and presence of carbon) greatly affect the microstructural development (e.g. wetting of the AlN grains by oxide phases).

The matrix part of the microstructure of type II samples was modelled and thermal conductivity was derived analogously as described for the type I samples, yet without the grain edge channels. The modelling is shown in Fig. 7, the resulting formula is given in Appendix 3. The dispersed Y aluminate grains were modelled by isolated spheres. The influence of such spheres on thermal conductivity was calculated using Bruggeman's formula,[15] see Appendix 4. The results of these calculations are given by the graphs in Fig. 8; measured values of thermal conductivity, oxygen content in the AlN lattice and amount of secondary phases are listed in Table 2.

The derivations of the formulae given in Appendices 2–4 are shown in Ref. 16.

3.2 Thermal conductivity of type I samples: comparison of measured values and modelling

Measured thermal conductivities of all samples are below the values calculated from the measured amounts of grain edge phases and the measured contents of oxygen in the AlN lattice (solid lines in Figs 4 and 5). They are very close to the conductivities calculated for an additional grain boundary phase of 2 nm thickness (dashed lines in Figs 4 and 5), the value that has been found analytically by TEM observation (see Fig. 3).

Figure 4 shows that the level of thermal conductivity of samples made from powder mixtures with

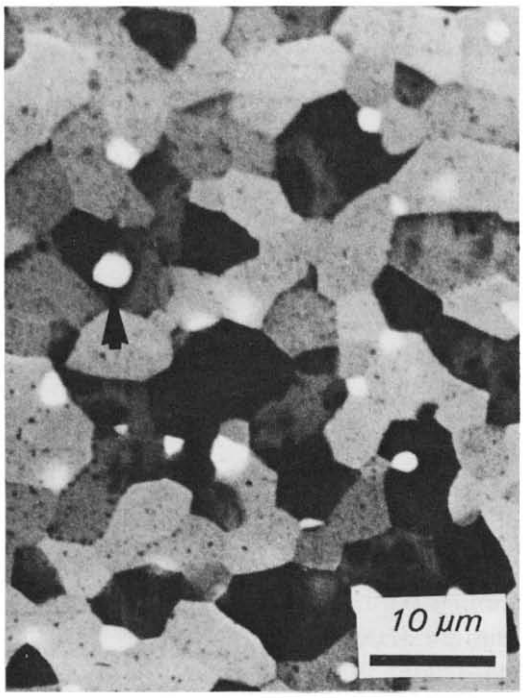

(a)

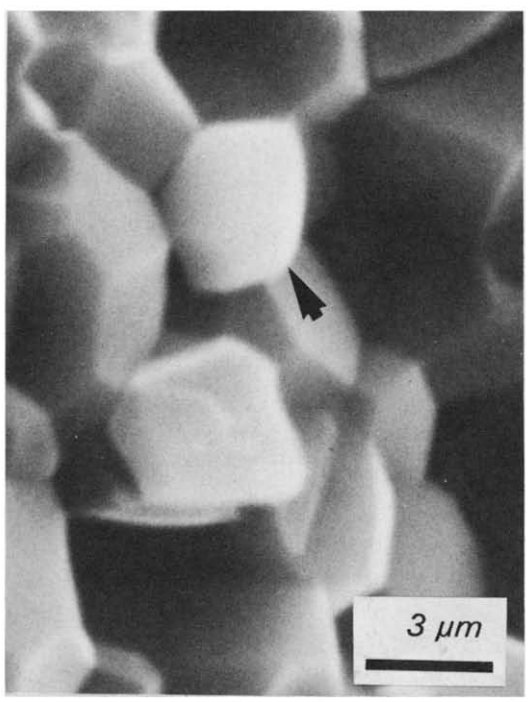

(b)

Fig. 6. SEM micrographs of AlN (3 wt% Y_2O_3) ceramic sintered in a graphite-free furnace. (a) Polished microsection showing that the Y aluminates are dispersed as isolated, rounded lumps (arrow); (b) fracture surface showing that the Y aluminates (arrow) are not wetting the AlN grains.

different amounts of additive (1–5 wt% Y_2O_3) is correlated with the oxygen content dissolved in the AlN lattice: a decreasing oxygen content of samples 1 to 4 in Fig. 4 leads to an increasing thermal conductivity, in spite of the concomitant increase of the amount of the grain edge phases. The maximum of thermal conductivity of sample 4 is due to the lowest oxygen content in the AlN lattice (0·1 wt%).

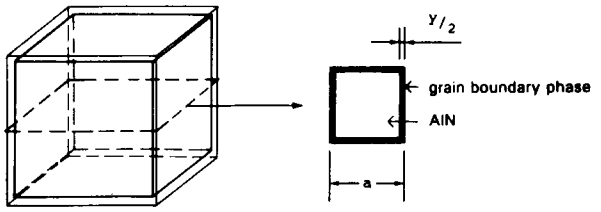

Fig. 7. Model of the AlN matrix phase of ceramics sintered in a graphite-free furnace.

This can be explained by an extraction mechanism of oxygen from the AlN lattice equilibrating the Al_2O_3 content in the AlN crystals with the Y aluminate phases.[3] The higher amount of grain edge phases explains the decrease in thermal conductivity of sample 5.

The decrease in thermal conductivity because of the increase in the amount of poorly conducting secondary phases (Y aluminates)—for a given oxygen content in the AlN lattice—is even more pronounced in the samples made from AlN powders with different overall oxygen contents (see Fig. 5). The oxygen content in the AlN lattice was very low (0·08–0·15 wt%) for all samples, as determined by hot gas extraction analysis (see Table 1). This is the result of Y_2O_3 concentrations (5·8 wt%, 9·2 wt% and 14·2 wt% for samples made of A, B and C powder), giving the same Al_2O_3/Y_2O_3 ratio as the mixture of the TSF powder with 4 wt% Y_2O_3. Again, measured thermal conductivities and calculated values are close together (see Fig. 5). Because of the detrimental influence of the secondary phases a high thermal conductivity of approximately 180 W/(m K) can only be reached by using a relatively oxygen-free AlN powder (total oxygen content < 1 wt%), if the samples are sintered within a short period of time (3 h).

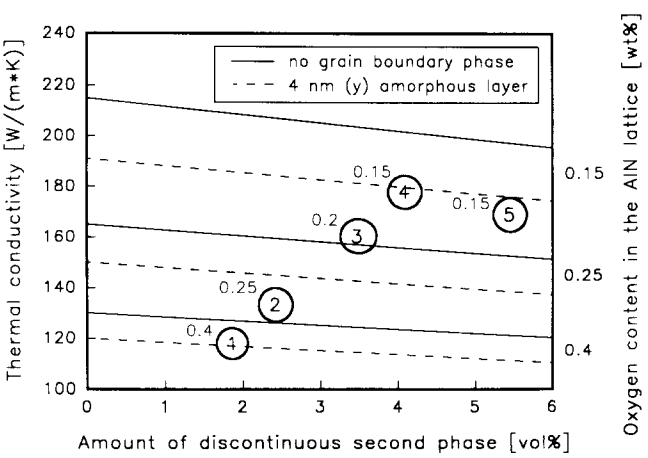

Fig. 8. Thermal conductivity as a function of the amount of grain edge phase. Parameters: oxygen content in the AlN lattice, width of grain boundary phase. Measured values: points 1–5 represent measured thermal conductivities and amount of grain edge phases of AlN ceramics with 1–5 wt% Y_2O_3 sintered at 1800°C for 3 h in a graphite-free furnace. The figures beside the data points give the measured oxygen contents in the AlN lattice in wt%.

Table 1. Thermal conductivity, total oxygen content, oxygen content in the AlN lattice and amount of grain edge phases of type I samples (esd of last digit given in parentheses)

AlN powder	*Oxygen in AlN powder (wt%)*	*Green bodies*		*Sintered bodies*			
		Amount Y_2O_3 (wt%)	*Total oxygen (wt%)*	*Thermal conductivity (W/(m K))*	*Total oxygen (wt%)*	*Oxygen in AlN lattice (wt%)*	*Grain edge phases (vol.%)*
TSF	0·85(1)	1·0	1·17(1)	130(4)	0·85(1)	0·31(3)	1·7(6)
TSF	0·85(1)	2·0	1·50(1)	146(4)	0·91(1)	0·24(3)	2·1(6)
TSF	0·85(1)	3·0	1·65(1)	165(5)	1·12(1)	0·19(3)	3·0(8)
TSF	0·85(1)	4·0	1·83(1)	185(6)	1·26(1)	0·12(3)	3·5(8)
TSF	0·85(1)	5·0	2·05(1)	171(5)	1·52(1)	0·13(3)	4·3(9)
TSF	0·85(1)	4·0	1·83(1)	185(5)	1·26(1)	0·12(3)	3·5(8)
A	1·40(1)	5·8	2·66(1)	165(5)	2·23(1)	0·13(3)	4·9(9)
B	2·20(1)	9·2	3·99(1)	158(5)	2·98(1)	0·08(3)	6(1)
C	3·40(1)	14·2	6·26(1)	153(5)	3·45(1)	0·15(3)	9(1)

3.3 Thermal conductivity of type II samples: comparison of measured values and modelling

The measured thermal conductivities of samples sintered in the graphite-free furnace are also close to the calculated values (points 1 to 5 and dashed line in Fig. 8). Again, it seems that the thermal conductivity is mainly influenced by the oxygen content dissolved in the AlN lattice. Thermal conductivities of these samples are lower than the conductivities of type I samples, because they have a higher amount of secondary phases (compare Tables 1 and 2). This is due to the absence of carbothermal reduction[3] in a graphite-free furnace. Indeed, the overall content of oxygen in the samples was found to be the same as in the green bodies (compare Tables 1 and 2). Consequently, thermal conductivity of these samples is mainly influenced by the Al_2O_3/Y_2O_3 ratio of the starting mixture and should be rather insensitive to sintering conditions.

4 Summary and Conclusions

Based on simple microstructural models thermal conductivities of AlN ceramics can be calculated. The model calculations and the measured values show that the oxygen dissolved in the AlN lattice has the dominating influence on thermal conductivity. The amount and thermal conductivity of a secondary phase along the grain edges or as isolated lumps only has a major influence on thermal conductivity if the oxygen content in the AlN grains is very low and if the amount of the secondary phase is rather high. Grain face layers strongly decrease thermal conductivity if they are thicker than a few nm or if their thermal conductivity is much lower than 1 W/(m K).

The measured thermal conductivities and the calculated values are in a good agreement: the deviations typically are < 15 W/(m K). This indicates that the simple modelling correctly reflects the fundamental correlations and it shows that the values chosen for the adaptable parameters of the model (thermal conductivity of the grain edge and grain face layers and thickness of the grain face layers) are reasonable. Better characterisation, particularly of the grain face layers, their thickness, composition and properties, and more precise data for the concentration of the lattice dissolved oxygen are still needed, in order to further test and improve the models. Expansion of these models to other microstructures and additional influences on thermal conductivity (e.g. impurities other than oxygen) should present no major problem.

Table 2. Thermal conductivity, total oxygen content, oxygen content in the AlN lattice and amount of grain edge phases of type II samples (esd of last digit given in parentheses)

AlN powder	*Oxygen in AlN powder (wt%)*	*Green bodies*		*Sintered bodies*			
		Amount Y_2O_3 (wt%)	*Total oxygen (wt%)*	*Thermal conductivity (W/(m K))*	*Total oxygen (wt%)*	*Oxygen in AlN lattice (wt%)*	*Grain edge phases (vol.%)*
TSF	0·85(1)	1·0	1·15(1)	121(4)	1·23(1)	0·40(3)	1·9(6)
TSF	0·85(1)	2·0	1·50(1)	135(4)	1·50(1)	0·26(3)	2·5(6)
TSF	0·85(1)	3·0	1·65(1)	159(5)	1·57(1)	0·19(3)	3·5(8)
TSF	0·85(1)	4·0	1·83(1)	175(6)	1·77(1)	0·12(3)	4·1(9)
TSF	0·85(1)	5·0	2·05(1)	163(5)	2·11(1)	0·15(3)	5·5(9)

Acknowledgements

The authors are grateful to Prof. T. Reetz for carrying out the sintering in the graphite-free furnace at the Bergakademie Freiberg, Germany and to Hoechst AG, Frankfurt, Germany for the measurements of the thermal conductivity. This work was supported by the Bundesminister für Forschung und Technologie of the Federal Republic of Germany under Grant No. 03M27020. The contents of the paper are the responsibility of the authors.

References

1. Slack, G. A., Tanzilli, R. A., Pohl, R. O. & Vandersande, J. W., The intrinsic thermal conductivity of AlN. *J. Phys. Solids*, **48** (1987) 641–7.
2. Slack, G. A., Nonmetallic crystals with high thermal conductivity. *J. Phys. Chem. Solids*, **34** (1973) 321–35.
3. Buhr, H., Müller, G., Wiggers, H., Aldinger, F., Foley, P. & Roosen, A., Phase composition, oxygen content and thermal conductivity of AlN (Y_2O_3) ceramics. *J. Am. Ceram. Soc.*, **74** (1991) 718–23.
4. Shinozaki, K., Iwase, N. & Tsuge, A., High thermal conductive aluminium nitride (AlN) substrates. FC Annual Report 1986 of Toshiba Research and Development Center, 1986, pp. 16–22.
5. Virkar, A. V., Jackson, T. B. & Cutler, A., Thermodynamic and kinetic effects of oxygen removal on the thermal conductivity of aluminum nitride. *J. Am. Ceram. Soc.*, **72** (1989) 2031–42.
6. Okamoto, M., Arakawa, H., Oohashi, M. & Ogihara, S., Effect of microstructure on thermal conductivity of AlN ceramics. *J. Ceram. Soc. Jpn Inter. Edn.*, **97** (1989) 1486–93.
7. Ruckmich, S., Kranzmann, A., Bischoff, E. & Brook, R. J., A description of microstructure applied to the thermal conductivity of AlN substrate materials. *J. Eur. Ceram. Soc.*, **7** (1991) 335–41.
8. Kurokawa, Y., Utsumi, K. & Takamizawa, H., Development and microstructural characterization of high-thermal-conductivity aluminium nitride ceramics. *J. Am. Ceram. Soc.*, **71** (1988) 588–94.
9. Yoneda, Y., Takaoka, T., Takeshima, Y., Sakabe, Y., Kasanami, T. & Wakino, K., Preparation of high thermal conductivity AlN ceramics and metallisation. In *IMC Proceed.*, Tokyo, 1988, pp. 147–52.
10. Clarke, D. R., On the detection of thin intergranular films by electron microscopy. *Ultramicroscopy*, **4** (1979) 33–44.
11. Thomas, A. & Müller, G., Determination of the oxygen concentration dissolved in the AlN lattice by hot gas extraction from AlN ceramics. *J. Eur. Ceram. Soc.*, **8** (1991) 11–19.
12. Sternitzke, M. & Müller, G., EELS analysis of AlN ceramics. In *Presentation (C15) of the 2nd Conference of Europ. Ceram. Soc. (ECerS)*, Augsburg, 1991. Proc. Vol. 3 (A: Electroceramics), 1855–1860, ed. G. Ziegler and H. Hausner.
13. Wiener, O., Lamellare Doppelbrechung. *Phys. Zeitschr.*, **5** (1904) 332–8.
14. Klein, P. H. & Croft, W. J., Thermal conductivity, diffusivity, and expansion of Y_2O_3, $Y_3Al_5O_{12}$, and LaF_3 in the range of 77–300 K. *J. Appl. Phys.*, **38** (1967) 1603–7.
15. Bruggeman, D. A. G., Berechnung verschiedener physikalischer Konstanten von heterogenen Substanzen, I. Dielektrizitätskonstanten und Leitfähigkeiten der Mischkörper aus isotropen Substanzen. *Ann. Physik*, **5** (1935) 636–64.
16. Buhr, H., Untersuchungen zur Wärmeleitfähigkeit von drucklos gesinterten AlN(Y_2O_3)-Keramiken. Dissertation, Technische Hochschule Darmstadt, FRG, 1992.

Appendix 1—Wiener's Formulae for Thermal Conductivity of a Composite Material

Parallel arrangement

$$\lambda_P = c_1 \cdot \lambda_1 + c_2 \cdot \lambda_2$$

Serial arrangement:

$$\lambda_S = (c_1/\lambda_1 + c_2/\lambda_2)^{-1}$$

where c_1 and c_2 = volume fraction of each component and λ_1 and λ_2 = thermal conductivity of each component.

Appendix 2—Formula for the Calculations of Thermal Conductivity (λ) of the Modelled Microstructure with Grain Edge Phase and Grain Boundary Phase[16]

$$\lambda = \frac{x^2}{2a^2} \cdot \lambda_{GE} + \frac{(a-x)^2}{a} \cdot \frac{\lambda_{AlN} \cdot \lambda_{GB}}{y \cdot \lambda_{AlN} + a \cdot \lambda_{GB}} + \frac{3x}{4a} \cdot \frac{\lambda_{AlN} \cdot \lambda_{GE}}{\lambda_{AlN} + (3a/2x - 1) \cdot \lambda_{GE}} + \frac{2x(a-x)}{a} \cdot \frac{\lambda_{AlN} \cdot \lambda_{GE}}{(x/2) \cdot \lambda_{AlN} + (a - x/2) \cdot \lambda_{GE}}$$

where a = length of cube edges, x = width of grain edge phase, y = thickness of grain boundary phase (see Fig. 3), λ_{AlN} = thermal conductivity of AlN, λ_{GE} = thermal conductivity of grain edge phase and λ_{GB} = thermal conductivity of grain boundary phase.

Simplifications: $(a-y) \approx a$; heat conduction of the grain boundary phase parallel to the direction of the heat flow is neglected. Differences of the total heat conduction between the values calculated by the formula without these simplifications and by the simplified formula used here are below 1 W/(m K).

Appendix 3—Thermal Conductivity of AlN Matrix Phase (λ_{matrix})[16]

$$\lambda_{matrix} = \frac{(a-y)}{a} \left[\frac{\lambda_{AlN} \cdot \lambda_{GB} \cdot (a-y)}{y \cdot \lambda_{AlN} + (a-y) \cdot \lambda_{GB}} + \frac{y}{a} \cdot \lambda_{GB} \right]$$

where a = length of cube edges, y = thickness of grain boundary phase (see Fig. 7), λ_{AlN} = thermal conductivity of AlN and λ_{GB} = thermal conductivity of grain boundary phase.

Appendix 4—Bruggeman's Formula[15] for Thermal Conductivity (λ) of a Composite Material of Spheres in a Continuous Matrix

$$1 - c_1 = \left[\frac{\lambda_2}{\lambda} \right]^{1/3} \cdot \frac{\lambda_1 - \lambda}{\lambda_1 - \lambda_2}$$

where c_1 = volume fraction of dispersed spheres, λ_1 = thermal conductivity of spheres and λ_2 = thermal conductivity of matrix phase.